

Critical evaluation of global mechanisms of wood devolatilization

Carmen Branca, Alessandro Albano, Colomba Di Blasi*

Dipartimento di Ingegneria Chimica, Università degli Studi di Napoli "Federico II", P.le V. Tecchio, 80125 Napoli, Italy

Received 11 November 2004; received in revised form 14 February 2005; accepted 25 February 2005

Available online 13 April 2005

Abstract

Thermogravimetric data on the devolatilization rate of beech wood are re-examined with the aim of incorporating the effects of high heating rates (up to 108 K min^{-1}) in the global kinetics. The mechanism consisting of three independent parallel reactions, first-order in the amount of volatiles released from pseudo-components with chief contributions from hemicellulose, cellulose and lignin, is considered first. It is found that the set of activation energies estimated by Gronli et al. [M.G. Gronli, G. Varhegyi, C. Di Blasi, *Ind. Eng. Chem. Res.* 41 (2002) 4201–4208] (100 , 236 and 46 kJ mol^{-1} , respectively) for one slow heating rate results in very high deviations between predicted and measured rate curves. The agreement is significantly improved by a new set of data consisting of activation energies of 147 , 193 and 181 kJ mol^{-1} , respectively. In this case, the overlap is reduced between the reaction rates of the three pseudo-components whose chemical composition is also modified. In particular, instead of a slow decomposition rate over a broad range of temperatures, the activity of the third reaction is mainly explicated along the high-temperature (tail) region of the weight loss curves. The performances of more simplified mechanisms are also evaluated. One-step mechanisms, using literature values for the kinetic constants, produce large errors on either the conversion time (activation energy of 103 kJ mol^{-1}) or the maximum devolatilization rate (activation energy of 149 kJ mol^{-1}). On the other hand, these parameters are well predicted by two parallel reactions, with activation energies of 147 and 149 kJ mol^{-1} .

© 2005 Elsevier B.V. All rights reserved.

Keywords: Kinetics; Wood; Devolatilization

1. Introduction

Thermogravimetric curves of wood/biomass pyrolysis, obtained under dynamic conditions and slow heating rates, show the presence of several reaction zones, resulting from the composite nature of the fuel. The majority of the kinetic models is based on three independent parallel reactions, first-order in the amount of volatiles released from hemicellulose, cellulose and lignin [1–3]. In reality, owing to the difficulty in separating the effects of the different contributions, these are pseudo-components. Following previous analyses [1–3], it is generally assumed that hemicellulose and cellulose decompose independently of one another, the former associated with the shoulder and the latter with the peak of the rate

curves. Lignin decomposes slowly over a very broad range of temperatures.

Dynamic measurements and the corresponding kinetic analyses have been based, for a large part, on the examination of one heating rate only, generally below 10 K min^{-1} . The agreement between the kinetic parameters, estimated by means of differential (DTG) curves, is good [1–7]. Activation energies vary between 80 and 116 kJ mol^{-1} for hemicellulose, 195 and 286 kJ mol^{-1} for cellulose, and 18 and 65 kJ mol^{-1} for lignin. Furthermore, the component contributions, expressed as percent of the total mass fraction, are roughly 20–30% for hemicellulose, 28–38% for cellulose and 10–15% for lignin.

The simultaneous evaluation of thermogravimetric curves obtained for several heating rates has been examined only in a few cases, which include 2 – 25 K min^{-1} for olive stones and almond shells [8], 3 – 100 K min^{-1} for untreated and water-washed rice husks [9], 0.5 – 108 K min^{-1} for water-washed

* Corresponding author. Tel.: +39 081 7682232; fax: +39 081 2391800.
E-mail address: dibiasi@unina.it (C. Di Blasi).

beech wood [10], and 5–20 K min⁻¹ for waste wood and other residues [11]. Apart from the different fuels and pre-treatments examined, the comparison between the results is difficult owing to power law dependences on the mass fraction [8,10,11], the use of integral (TG) data only [9–11] and the selection of widely different values of the component fractions. The overall trend is that the kinetic evaluation of cellulose remains roughly unchanged (activation energies of 192–250 kJ mol⁻¹) with respect to single-curve results, whereas higher activation energies of hemicellulose degradation are reported (154–200 kJ mol⁻¹). As for the reaction of the third component, activation energies of 36 kJ mol⁻¹ [9], 188 kJ mol⁻¹ [8], or 54–61 kJ mol⁻¹ [11] have been estimated (in [10] the degradation of the third component takes place along the low-temperature region typical of hemicellulose and, therefore, the related kinetic constants cannot be referred to the lignin component). Hence, it is not clear whether the three component mechanism, as originally proposed by Antal and Varhegyi [2] and also applied [1] to a high number of wood species for a heating rate of 5 K min⁻¹, could also be valid for predicting the devolatilization rates over a wide range of heating rates and/or how the kinetic constants should be modified. The inclusion of several heating rates, especially the higher values, in kinetic analysis of wood/biomass devolatilization is important from both the theoretical and the practical side. Indeed, the evaluation of multiple curves is proposed as a mean to break the compensation effect [12]. Moreover, the fuel particles in industrial systems usually experience widely variable heating rates, generally barely touched by the upper limits of thermal analysis.

The three-step mechanism discussed here provides a description of the global devolatilization rates of the three wood pseudo-components. Other mechanisms, which also include the evaluation of the rates of char formation and, thus, the variation in the ratio between the volatile and char yields, have been discussed in the literature review presented in [13,14]. The most widely used mechanism consists of three parallel reactions [15] for the formation of the main classes of wood pyrolysis products (char, gases and liquids). In this case it is implicitly assumed that devolatilization is a one-step process as the activation energies for the reactions of liquid and gas formation are comparable. The inaccuracies introduced by this simplification in the prediction of the dynamics of weight loss and/or their abilities to predict correctly at least global parameters, such as the conversion time and the maximum devolatilization rate, have not been evaluated.

In this study, thermogravimetric curves of beech wood are used to understand the dependence of the devolatilization characteristics on the heating rate. Then, the performances of devolatilization mechanisms, consisting of one, two or three parallel reactions are evaluated for the predictions of both the details of the weight loss curves and the global devolatilization parameters. Also, new kinetic constants are estimated, where appropriate.

2. Thermogravimetric curves and kinetic modeling

The examination of the effects of the heating rate on the global kinetics of wood devolatilization in inert atmosphere is carried out by means of thermogravimetric curves already available in the literature for beech wood (*Fagus sylvatica*). The first set of thermogravimetric curves is derived from [16], whose authors worked with about 20 mg of (untreated) wood (particles in the range 0.3–0.85 mm) with heating rates of 5, 20 and 80 K min⁻¹. It should be noted that these data were used to propose a two-stage mechanism (an activation step followed by two competitive reactions for the formation of char and volatiles, respectively) for each of the main components of wood. The second set of data is derived from [10], whose authors examined about 3 mg of extracted (hot water) wood (particles below 0.5 mm) with heating rates of 3, 41 and 108 K min⁻¹. Both sets of thermogravimetric curves were measured with commercial systems (Mettler TA 300 [16] and STA 500 Bahr GmbH [10]) and only weight loss (integral) data were provided. These have been numerically differentiated to obtain rate curves. In the following, the first [16] and second [10] set of thermogravimetric data will be referred to as untreated and water-washed wood, respectively.

A kinetic model of wood devolatilization, widely used in previous literature (for instance, [1–7]), assumes that the total volatiles released consist of m fractions, whose dynamics are described by first order kinetics. Then, the overall mass loss rate is a linear combination of the single fraction rates. More specifically, the mechanism consists of m independent parallel reactions:



In the majority of the devolatilization mechanisms, the C_i are assumed to be the volatile contents of the three pseudo-components corresponding mainly to hemicellulose, cellulose and lignin, respectively (V_i are the corresponding lumped volatile species generated). In a few cases, additional fractions have been introduced, for instance, to take into account moisture evaporation [9] or the dynamics of extractive decomposition [1]. Three cases will be considered in the following corresponding to $m = 3, 2$ and 1 (three-, two- and one-step mechanisms), though the model equations given below are for the first case.

The reactions rate is assumed to present the usual Arrhenius dependence (A_i are the pre-exponential factors and E_i , the activation energies) on temperature and to be proportional to the mass fractions, Y_i , of components C_i :

$$R_i = A_i \exp\left(\frac{-E_i}{RT}\right) Y_i, \quad i = 1, 3 \quad (1-3)$$

As the sample temperature, T , is a known function of time, t :

$$T = T_0 + ht \quad (4)$$

(T_0 is the initial temperature and h), the heating rate, the mathematical model can be expressed as:

$$\frac{\partial Y_i}{\partial t} = -R_i, \quad Y_i(0) = v_i, \quad i = 1, 3 \quad (5-7)$$

where v_i , indicated in the following as stoichiometric coefficients, are the initial mass fractions of the volatile content of the three pseudo-components.

The kinetic parameters are estimated through the numerical solution (implicit Euler method) of the mass conservation equations and the application of a direct method for the minimization of the objective function, which considers the differential (DTG) data. The details of the method, already described elsewhere (see, for instance, [17]), can be summarized as follows. It is a method belonging to the class of comparison methods, used to find the minimum of a scalar function of n independent variables. In contrast to gradient methods, direct methods do not require the derivatives of the scalar function. An approach combining the Rosenbrock formulas and the golden section method is used for selecting the orientation of the axis along which the optimum of the objective function should be found. The objective function, F , can be expressed as:

$$F = \sum_{j=1, M} f_j \sum_{i=1, N} \left[\frac{(dY_{ij})_{\text{exp}} - (dY_{ij})_{\text{sim}}}{(dY_{ij})_{\text{exp}} + (dY_{ij})_{\text{sim}}} \right]^2 \quad (8)$$

where i represents the experimental (exp) or simulated (sim) time derivative (dY) the solid mass fraction at time t ; j , the heating rate (N is the number of experimental points and M , the number of experiments carried out for each sample by varying the heating rate); and the scale parameter, f_j , is expressed as

$$f_j = \frac{1}{\max_j [(dY_{ij})_{\text{exp}}]^2} \quad (9)$$

The parameters to be estimated are the activation energies (E_i , $i = 1, 3$), the pre-exponential factors (A_i , $i = 1, 3$), and the stoichiometric coefficients (v_i , $i = 1, 2$), given the relation

$$\sum_{i=1, 3} v_i = 1 - Y_{C\infty} \quad (10)$$

where $Y_{C\infty}$ is the final char yield, that can be obtained from the measured curves.

The devolatilization mechanism (a1–a3) does not take into account the competition between volatile and char formation as the reaction temperature is varied. Therefore, while the pre-exponential factors and activation energies are invariant, the stoichiometric coefficients (Eqs. (5–7)) can vary with the heating conditions, to describe the decrease in the final yield of char for increasing reaction temperature. In other words, the devolatilization mechanisms can only predict the devolatilization rate, given the total amount of volatiles generated from the measured weight loss curves (see Eq. (10)).

The deviation between measured and calculated curves is defined in accordance with previous analyses [1] as:

$$\text{Dev} (\%) = \frac{\sqrt{S/N}}{(-dY/dt_k)_{\text{exp, peak}}} \times 100 \quad (11)$$

$$S = \sum_{k=1, N} \left(\left(\frac{-dY}{dt_k} \right)_{\text{exp}} - \left(\frac{-dY}{dt_k} \right)_{\text{sim}} \right)^2 \quad (12)$$

where k represents the experimental (exp) or the simulated (sim) devolatilization rate at time t (N is the number of experimental points (200 for the results discussed below) and the subscript peak indicates the maximum value). The application of the estimation procedure to multiple curves, obtained for several heating rates, allows the compensation effect to be avoided. Indeed, only one set of data can predict the behavior of the material at several heating rates, consisting of the displacement of the weight loss curves toward successively higher temperatures for successively more severe thermal conditions. Finally, it should be noted that, though in a few cases three consecutive reactions have been proposed (for instance, [14]), a parallel mechanism has been preferred here because of its higher flexibility.

3. Results

The thermogravimetric curves of wood are used first to evaluate the effects of the heating rate on the devolatilization characteristics and then for a kinetic analysis based on different mechanisms.

3.1. Influences of the heating rate on the devolatilization characteristics

The qualitative dependence of the weight loss curves of wood pyrolysis on the reaction temperature has already been extensively discussed in the literature (see, for instance, [1]). In order to quantify the effects of the heating rate on the degradation process, the same parameters introduced by Gronli et al. [1] have been evaluated and reported in Tables 1 and 2. They are related to the characteristic temperatures of the different zones of the weight loss curves and the corresponding mass fractions and devolatilization rates. The initial degradation temperature, T_{initial} , corresponds to a solid mass fraction equal to 0.975. The beginning of hemicellulose decomposition is associated with $T_{\text{onset(hc)}}$ defined by extrapolating the slope of the devolatilization rate in correspondence of the first local maximum in $-d^2Y/dt^2$ (up to the zero level of the Y -axis). Given the appearance of a shoulder, the decomposition temperature of the hemicellulose is characterized by T_{shoulder} , defined by the point where $-d^2Y/dt^2$ attains the value nearest to zero in this region. For the cases when the hemicellulose and cellulose decomposition is less overlapped, the parameter T_{shoulder} marks the peak top of the hemicellulose decomposition. The corresponding devolatilization

Table 1
Degradation characteristics of wood: temperatures (experimental measurements from [10,16])

h (K min ⁻¹)	Pre-treatment	T_i (K)	$T_{\text{onset}(hc)}$ (K)	T_{shoulder} (K)	T_{peak} (K)	$T_{\text{offset}(c)}$ (K)	$T_{\text{shoulder}} - T_{\text{onset}(hc)}$	$T_{\text{offset}(c)} - T_{\text{peak}}$
5	Untreated	523	512	572	619	646	64	27
20	Untreated	538	534	589	639	666	55	27
80	Untreated	548	546	601	668	688	54	20
3	H ₂ O-washed	524	513	561	623	642	48	19
41	H ₂ O-washed	539	565	606	670	693	41	24
108	H ₂ O-washed	562	574	628	689	713	54	24

Table 2
Degradation characteristics of wood: mass fractions and devolatilization rates (experimental measurements from [10,16])

h (K min ⁻¹)	Pre-treatment	Y_{shoulder}	Y_{peak}	$Y_{\text{offset}(c)}$	Y_{∞}	$Y_{\text{offset}(c)} - Y_{\infty}$	$-(dY/dt)_{\text{shoulder}} \times 10^3$ (s ⁻¹)	$-(dY/dt)_{\text{peak}} \times 10^3$ (s ⁻¹)
5	Untreated	0.83	0.48	0.32	0.238	0.08	0.37	0.91
20	Untreated	0.84	0.5	0.29	0.22	0.07	1.21	3.48
80	Untreated	0.86	0.42	0.28	0.23	0.05	5	12.7
3	H ₂ O-washed	0.86	0.48	0.28	0.23	0.05	0.19	0.615
41	H ₂ O-washed	0.81	0.42	0.27	0.24	0.03	2.94	7
108	H ₂ O-washed	0.75	0.385	0.215	0.185	0.03	8	17.1

rate, $-(dY/dt)_{\text{shoulder}}$, and mass fraction, Y_{shoulder} , can be easily evaluated. The temperature T_{peak} , where the maximum devolatilization rate is attained (associated mainly with cellulose decomposition), is also introduced with the corresponding $-(dY/dt)_{\text{peak}}$ and Y_{peak} . The beginning of the final, tailing region dominated by the lignin decomposition, is identified by $T_{\text{offset}(c)}$, which is obtained by extrapolating the devolatilization rate corresponding to the local minimum of $-d^2Y/dt^2$ in this region (again up to the zero level of the Y -axis). Finally, $Y_{C\infty}$ is the char mass fraction for a temperature of 750 K, when the devolatilization process terminates.

The characteristic temperatures evaluated for the untreated beech at 5 K min⁻¹ are very close to those reported by Gronli et al. [1], though mass fractions are slightly different. Indeed, the degradation rates are slightly slower, as indicated by lower $-(dY/dt)_{\text{shoulder}}$ and higher Y_{peak} and $Y_{C\infty}$, plausibly as a consequence of the influences of sample origin or mass (20 mg versus 5 mg).

As the heating rate is increased, all the characteristic temperatures become successively higher (especially T_{peak} , as also observed in [9,18]). The displacement of the rate curve at higher temperatures is clearly shown, for example, by the DTG curves of untreated wood for 5 and 80 K min⁻¹ reported in Fig. 1. The maximum displacement is observed for T_{peak} (49 K) and the minimum for T_{shoulder} (20 K). As a consequence, the extension of the reaction zone is enlarged ($T_{\text{offset}(c)} - T_{\text{onset}(hc)}$ varies from 134 to 142 K) and the reactions take place at successively higher temperatures. Also, the hemicellulose shoulder and the lignin tail become less visible, so that the overlap between adjacent reaction zones is enhanced.

A plot of the characteristic reaction temperatures as functions of the heating rate (Fig. 2) clearly shows higher values for the second set of data (especially T_{peak} and $T_{\text{offset}(c)}$). This finding is also in agreement with previous literature [2,3]. Indeed, by reducing the inorganic content of the sample through

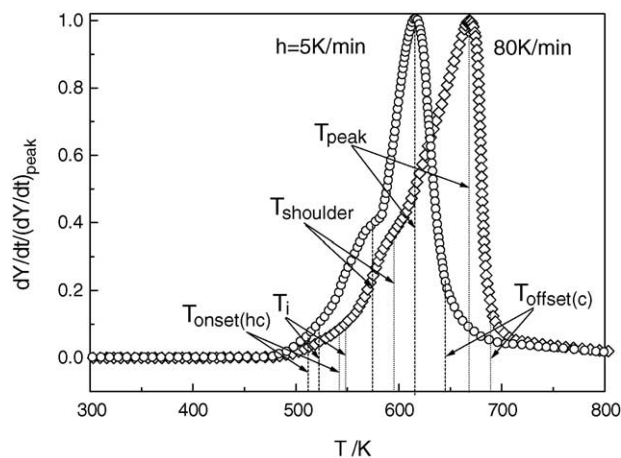


Fig. 1. Time derivative of the mass fraction, normalized with respect to the peak rate, with characteristic temperatures for heating rates of 5 and 80 K min⁻¹ (untreated beech wood [16]).

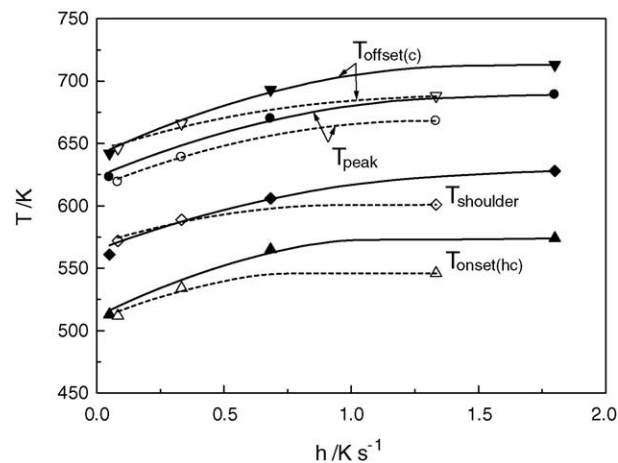


Fig. 2. Characteristic temperatures as functions of the heating rate for untreated (dashed lines [16]) and water-washed (solid lines [10]) beech wood.

water (or mild acid) washing, the cellulose peak is shifted at higher temperatures and a better separation is achieved between the hemicellulose and the cellulose zone. It is also worth noting that in this case, as the heating rate is increased, both the shoulder and the peak of the rate curves are displaced towards higher temperatures (maximum displacement of about 66 K). This behavior indicates that increases of the heating rate beyond 100 K min^{-1} do not introduce further changes in the reaction temperatures.

Given the high heating rates used in the thermogravimetric measurements [6,10], an approximate evaluation of possible heat/mass transfer intrusions has been carried out. Assuming a simple model based on one-step devolatilization reaction with activation energy E (that is, only the central zone of the rate curve, corresponding to the cellulose component, is responsible for the peak in the wood devolatilization rate), it can be shown [9] that, for a kinetically controlled process, the following relation holds:

$$Z = \frac{E}{R}h \quad (13)$$

$$Z = \frac{-(dY/dt)_{\text{peak}}}{Y_{\text{peak}}/T_{\text{peak}}^2} \quad (14)$$

In other words, the variable Z , a combination of the characteristic parameters evaluated in correspondence of the peak rate of the thermogravimetric curve, should present a linear dependence on the heating rate. As shown in Fig. 3, both sets of experimental data reproduce the trend described by Eqs. (13) and (14) with acceptable accuracy, indicating that they can be used for kinetic evaluation.

The estimated activation energy (about $92 \pm 9.5 \text{ kJ mol}^{-1}$) is about the half of that reported for the decomposition of the cellulosic component in wood. This result can be explained taking into account that cellulose may contribute up to a maximum of about 50% in the wood composition. For a one-step process, this appears as a reduction in the peak rate and con-

sequently in the estimated E value. On the other hand, the use of thermogravimetric curves of cellulose pyrolysis (heating rates in the range $0.5\text{--}108 \text{ K min}^{-1}$ [10] and $1\text{--}65 \text{ K min}^{-1}$ [19]) results in an activation energy of $209.7 \pm 4.6 \text{ kJ mol}^{-1}$ (Fig. 3), which is in the range of those obtained by means of accurate kinetic analysis.

3.2. Three-step mechanisms

The simultaneous evaluation of the differential curves for different heating rates, to estimate the kinetic parameters of the three-step mechanism a1–a3, has been carried out separately for the untreated and the water-washed samples. However, the optimization procedure has always been executed by requiring the same value of each activation energy, E_i , $i = 1, 3$, for all the curves (untreated and water-washed samples at different heating rates). The pre-exponential factor, A_i , is invariant with the heating rate but, as anticipated, the stoichiometric coefficients are allowed to vary.

In the first place, the activation energies for the three reactions have been assigned as those reported by Gronli et al. [1], that is, $E_1 = 100 \text{ kJ mol}^{-1}$, $E_2 = 236 \text{ kJ mol}^{-1}$ and $E_3 = 46 \text{ kJ mol}^{-1}$, and the other parameters have been estimated. The three-step mechanism a1–a3 and the set of kinetic parameters estimated in this way are indicated as model A. Results are summarized in Table 3, Figs. 4 and 5. The agreement between the measured and predicted global devolatilization rates is not acceptable for both untreated (Fig. 4) and water-washed (Fig. 5) wood, as also testified by the high deviations reported in Table 3. The stoichiometric coefficients ($\nu_1 = 0.25\text{--}0.30$, $\nu_2 = 0.38\text{--}0.44$ and $\nu_3 = 0.09\text{--}0.13$) are comparable with those previously obtained for slow heating rates [1].

Antal et al. [19], in their analysis of cellulose pyrolysis, attributed variations (by factors of 2–4) in the pre-exponential factors with the heating rate to uncontrolled systematic errors in the dynamic sample temperature measurements (thermal lag). Thus, in the case of model A, evaluations of the weight loss curves have also been made by removing the constraint of invariant pre-exponential factors (results not shown). The agreement between predictions and measurements is highly

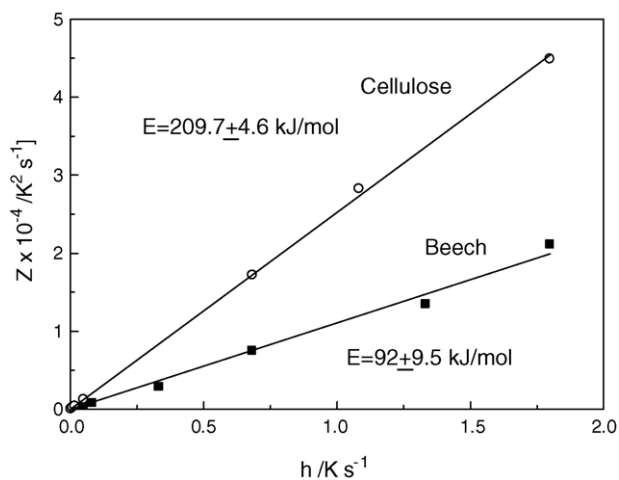


Fig. 3. Parameter Z (Eqs. (16) and (17)) as a function of the heating rate for cellulose [10,19] and beech [10,16].

Table 3

Parameters for the three-step devolatilization mechanism with activation energies as in Gronli et al. [1]

h (K min^{-1})	ν_1	ν_2	ν_3	Dev (%)
Untreated wood				
5	0.25	0.38	0.13	21.92
20	0.29	0.38	0.11	9.01
80	0.30	0.38	0.09	11.76
Water-washed wood				
3	0.23	0.44	0.10	22.05
41	0.27	0.42	0.06	7.56
108	0.28	0.42	0.11	18.64

E_1 (kJ mol^{-1}) = 100; E_2 (kJ mol^{-1}) = 236; E_3 (kJ mol^{-1}) = 46; A_1 (s^{-1}) = 6.84×10^6 ; A_2 (s^{-1}) = 2.91×10^{17} (1.41×10^{17} for water-washed wood); A_3 (s^{-1}) = 32.95.

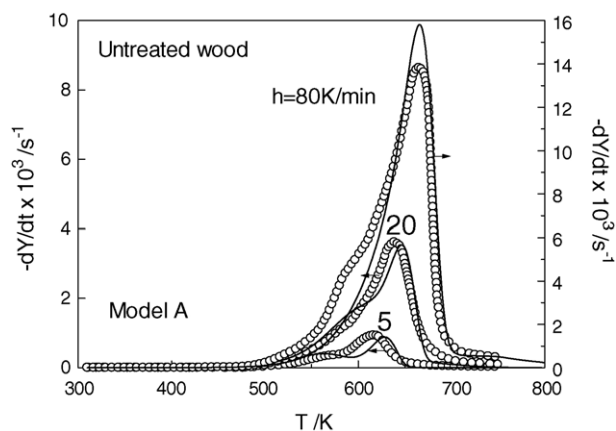


Fig. 4. Comparison between the observed (symbols) and simulated DTG curves (solid lines) for untreated beech wood [16] (model A, kinetic parameters listed in Table 3).

improved but, while the variations for the cellulose component are relatively small (diminution of A_1 by factors of 1.5–2.5), those for the hemicellulose and lignin components are very high (augmentation in A_2 and A_3 by factors of 4–5 and 11–21, respectively), as also found by Teng and Wei [9] (in this case $E_3 = 34\text{--}36\text{ kJ mol}^{-1}$ and A_3 varies by factors of 40–50). From this analysis, it appears that the activation energies for the three reactions, determined with only one slow heating rate, should be modified to improve the accuracy of the predictions when the thermal conditions are varied.

Following previous analyses, carried out for several heating rates, which list activation energies [8–11] for the hemicellulose and lignin components significantly different from those of model A, a new set of kinetic data has been estimated. In this case, the evaluation of the thermogravimetric curves has been carried out with no constraint on the activation energies for the reactions a1 and a3 (hemicellulose and lignin pseudo-components). For the reaction a2 (pseudo-component cellulose), given the huge amount of work done [2] and the general consensus about a one-step

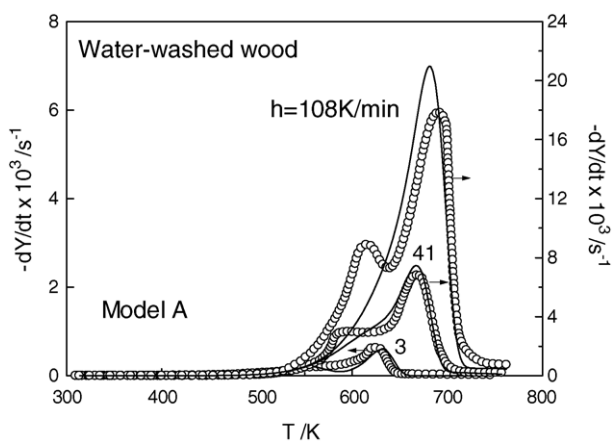


Fig. 5. Comparison between the observed (symbols) and simulated DTG curves (solid lines) for water-washed beech wood [10] (model A, kinetic parameters listed in Table 3).

Table 4

Parameters for the three-step devolatilization mechanism with kinetic parameters estimated in this study

h (K min ⁻¹)	ν_1	ν_2	ν_3	Dev (%)
Untreated wood				
5	0.18	0.46	0.12	3.20
20	0.18	0.48	0.12	4.31
80	0.20	0.49	0.08	6.61
Water-washed wood				
3	0.20	0.48	0.09	8.74
41	0.20	0.47	0.08	5.83
108	0.24	0.47	0.10	7.41

E_1 (kJ mol⁻¹) = 147; E_2 (kJ mol⁻¹) = 193; E_3 (kJ mol⁻¹) = 181; A_1 (s⁻¹) = 2.527×10^{11} ; A_2 (s⁻¹) = 1.379×10^{14} (5.493×10^{13} for water-washed wood); A_3 (s⁻¹) 2.202×10^{12} .

reaction with high activation energy, the range of variation has been limited to 190–240 kJ mol⁻¹ while applying the optimization procedure. The three-step mechanism a1–a3 and the set of kinetic parameters estimated in this way are indicated as model B. The results, summarized in Table 4, report the following activation energies: $E_1 = 147\text{ kJ mol}^{-1}$, $E_2 = 193\text{ kJ mol}^{-1}$ and $E_3 = 181\text{ kJ mol}^{-1}$. A small variation on the pre-exponential factor of the cellulose component can take into account the effects of water washing. Furthermore, the stoichiometric coefficients appear to increase (hemicellulose, $\nu_1 = 0.18\text{--}0.24$) or slightly decrease (lignin, $\nu_3 = 0.08\text{--}0.12$) with the pre-treatment, whereas those for cellulose (0.46–0.49) are roughly constant. It should be mentioned that several combinations of kinetic parameters have been tested and those associated with the lowest value of the objective function have been chosen (absolute minimum). Figs. 6 and 7, and the deviation values (Table 4) show that the agreement between the predicted and measured global rates is highly improved with respect to the three-step model A and the model results are acceptable.

Fig. 8A and B compare the component dynamics for the models A and B at two heating rates. Both models predict the same qualitative characteristics for the hemicellulose and

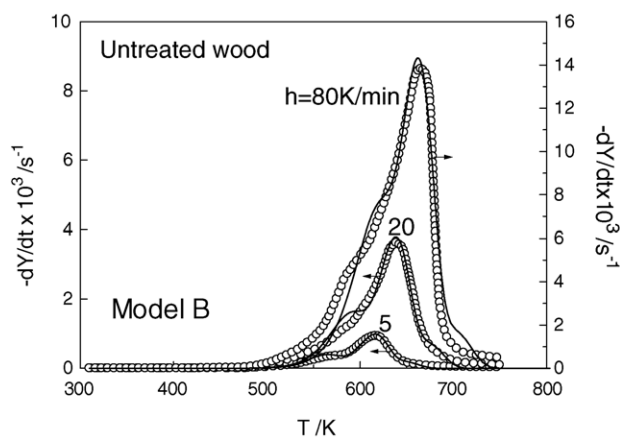


Fig. 6. Comparison between the observed (symbols) and simulated DTG curves (solid lines) for untreated beech wood [16] (model B, kinetic parameters listed in Table 4).

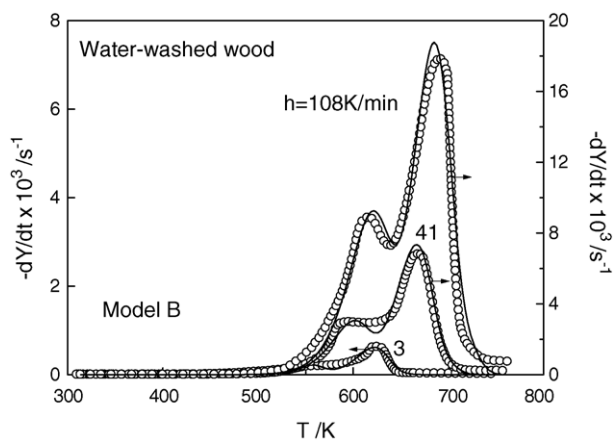
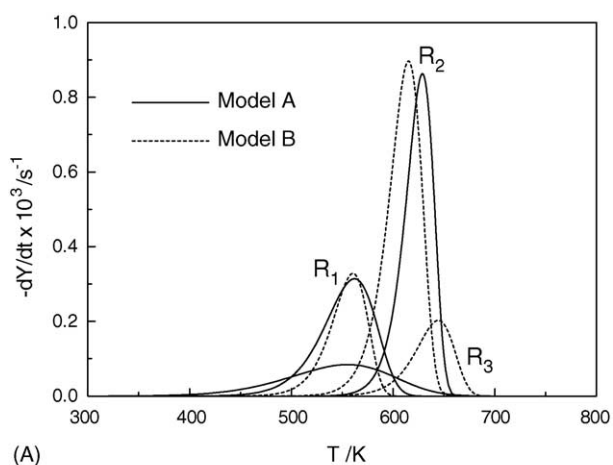
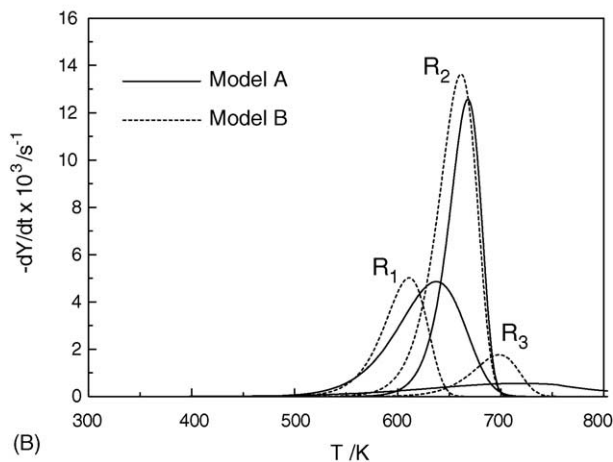


Fig. 7. Comparison between the observed (symbols) and simulated DTG curves (solid lines) for water-washed beech wood [10] (model B, kinetic parameters listed in Table 4).



(A)



(B)

Fig. 8. Predicted volatile evolution from the different components for models A (kinetic parameters listed in Table 3) and B (kinetic parameters listed in Table 4) for untreated beech wood and a heating rate of 5 K min^{-1} (A) and 80 K min^{-1} (B).

cellulose components, which describe the shoulder and peak of the rate curves, respectively. From the quantitative point of view, however, the volatile contribution from cellulose is augmented by the model B (0.47–0.49 versus 0.38–0.44). It is released over a slightly wider reaction zone, as also indicated by a diminution in the activation energy of this reaction (193 kJ mol^{-1} versus 236 kJ mol^{-1}). Conversely, the amounts of volatiles released from hemicellulose are reduced (0.17–0.20 of the model B versus 0.23–0.30 of the model A) together with the size of the reaction zone, as a consequence of the higher activation energy (147 kJ mol^{-1} versus 100 kJ mol^{-1}). The quantitative contribution from lignin is almost the same for both models (0.07–0.13 for the model A versus 0.08–0.12 of the model B) but the dynamics are highly different. Indeed, for the model B, the activity of this component is explicated essentially along the tail zone of the curve, whereas in the other case it slowly decomposes over a broad range of temperatures.

As a general remark, the overlap between the different reaction zones is reduced passing from models A to B, as if shifting from a parallel- to a series-reaction mechanism. Hence, in the model A, the three pseudo-components try to mimic the separate degradation rates of hemicellulose, cellulose and lignin over the entire temperature range where wood degradation takes place. In the model B, they tend to incorporate the simultaneous activity of all the wood components over three adjacent temperature ranges, but still including the maximum degradation rate of the single components (according to thermogravimetric analysis [20], hemicelluloses decompose over 498–598 K, cellulose over 598–648 K, and lignin over 523–773 K). In conclusion, the same conceptual mechanism of wood devolatilization (three parallel first order reactions) can be associated with pseudo-components with different chemical composition and kinetic parameters. However, while in the case of the model B, quantitative predictions can be obtained at both slow and fast heating rates, the model A, as extensively discussed in previous literature [1–7], appears to be accurate only for slow heating rates (upon adequate selection of pre-exponential factors).

3.3. One- and two-step mechanisms

Although it can be expected that a higher number of kinetic parameters, such as the introduction of a reaction order different from unity, an increase in the number of reaction steps in the devolatilization mechanism (a1–am) or the application of distributed activation energy models, would further improve the agreement between the predicted and measured details of the thermogravimetric curves, only a few global parameters are often required in practical applications. Indeed, in the majority of transport models, devolatilization is described by a global one-step reaction (for instance, [21,22]) or by two competitive reactions for the formation of gases and liquids (for instance, [23,24]). Based on the analysis of the literature and different mathematical treatments of isothermal weight loss measurements of

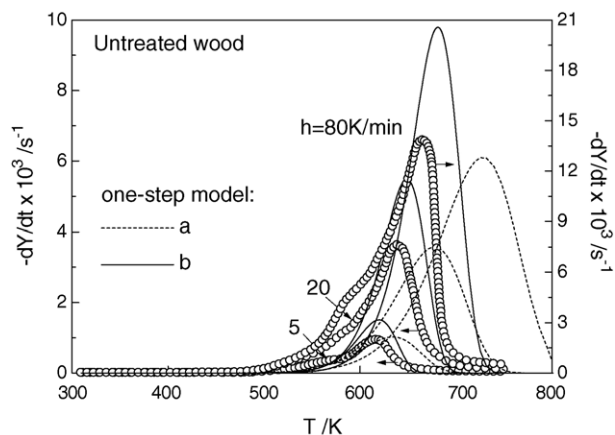


Fig. 9. Comparison between the observed (symbols) and simulated DTG curves (solid lines) for untreated beech wood [16] by means of a global one-step reaction (a) $E = 102.6 \text{ kJ mol}^{-1}$, $A = 7.71 \times 10^5 \text{ s}^{-1}$; (b) $E = 148.6 \text{ kJ mol}^{-1}$, $A = 1.45 \times 10^{10} \text{ s}^{-1}$ [13].

beech wood, it was shown [13] that two set of parameters can be estimated for a one-step devolatilization reaction: (a) $E = 102.6 \text{ kJ mol}^{-1}$, $A = 7.71 \times 10^5 \text{ s}^{-1}$ (low activation energy) and (b) $E = 148.6 \text{ kJ mol}^{-1}$, $A = 1.45 \times 10^{10} \text{ s}^{-1}$ (high activation energy). An example of the predictions obtained for the dynamic curves is shown in Fig. 9 for untreated wood, where measurements are also reported for comparison purposes (results are qualitatively similar for water-washed wood). It can be seen that the details of the curves are not predicted and large deviations (increasing with the heating rate) also occur for the global parameters, especially the conversion time (or temperature) for the case (a) and the maximum devolatilization rate for the case (b).

The applicability of a kinetic model, consisting of two parallel reactions, has also been evaluated for the prediction of the global devolatilization characteristics. The kinetic parameters of the first step have been assumed to coincide with those previously determined for the three-step model B. The second step has been assumed to present the same activation energy of the global one-step reaction *b* and the stoichiometric coefficient given by the sum of those for cellulose and lignin of the three-step model B. In this way, the pre-exponential factor for the second reaction has been estimated. The results are sum-

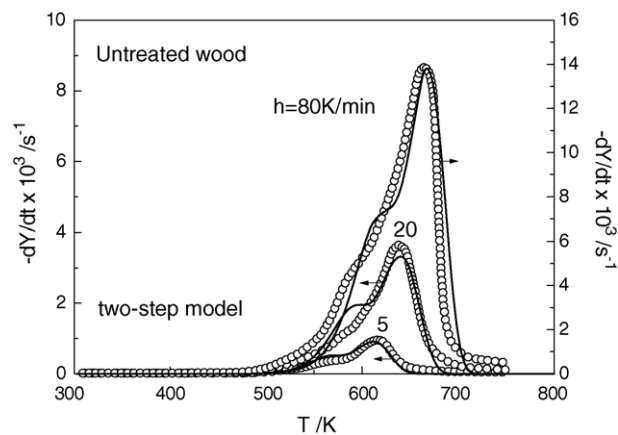


Fig. 10. Comparison between the observed (symbols) and simulated DTG curves (solid lines) for untreated beech wood [16] (two-step model, kinetic parameters listed in Table 5).

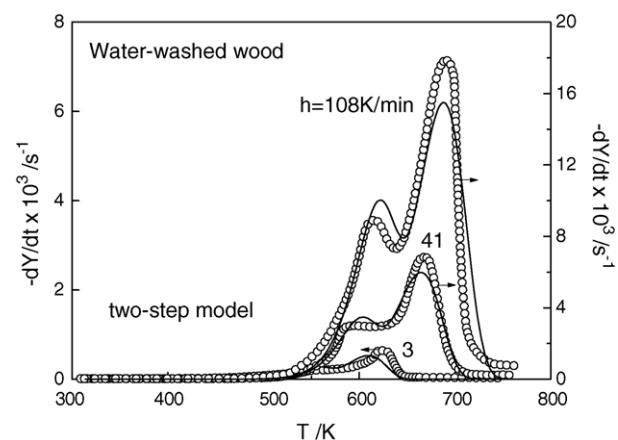


Fig. 11. Comparison between the observed (symbols) and simulated DTG curves (solid lines) for water-washed beech wood [10] (two-step model, kinetic parameters listed in Table 5).

marized in Table 5, Figs. 10 and 11. As expected, compared with the three-step model B (Table 4), the deviations between predictions and measurements are higher (Table 5). However, conversion times (temperatures), maximum devolatilization rates and times (temperatures) of maximum devolatilization rate are quantitatively correct.

Table 5

Parameters for the two-step devolatilization mechanism with kinetic parameters estimated in this study

$h \text{ (K min}^{-1}\text{)}$	ν_1	ν_2	Dev (%)
Untreated wood			
5	0.18	0.58	11.4
20	0.18	0.58	6.39
80	0.20	0.58	19.32
Water-washed wood			
3	0.20	0.57	26.3
41	0.20	0.55	6.31
108	0.24	0.57	11.79

$E_1 \text{ (kJ mol}^{-1}\text{)} = 146.7$; $A_1 \text{ (s}^{-1}\text{)} = 2.57 \times 10^{11}$; $E_2 \text{ (kJ mol}^{-1}\text{)} = 148.6$; $A_2 \text{ (s}^{-1}\text{)} = 1.45 \times 10^{10}$ (2.24×10^{10} for untreated wood).

4. Conclusions

Two sets of literature data on the devolatilization rate of beech wood have been re-examined with the aim of incorporating the effects of high heating rates (up to 108 K min^{-1}) in kinetic modeling. The model based on three independent parallel reactions, first-order in the amount of volatiles released from three pseudo-components with chief contributions from hemicellulose, cellulose and lignin, has been evaluated (three-step model).

A first kinetic evaluation has been made using the same activation energies (100 , 236 and 46 kJ mol^{-1} , respectively)

as in the unified model proposed by Gronli et al. [1] for nine wood species decomposing at a heating rate of 5 K min^{-1} . It has been found that this constraint does not allow acceptable predictions of the rate curves to be obtained for both untreated and water-washed wood. That is, the kinetics determined with one slow heating rate experiment are not valid when the thermal conditions are modified. A second kinetic evaluation has resulted in different activation energies (147, 193 and 181 kJ mol^{-1} , respectively) with good agreement between predictions and measurements. Relatively small variations on the stoichiometric coefficients and the pre-exponential factor of the cellulose pseudo-component can take into account sample pre-treatment effects. Both sets of kinetic data predict the same qualitative dynamics of the hemicellulose and cellulose pseudo-components, whereas those of the lignin pseudo-component are highly different. Indeed, the low activation energy (46 kJ mol^{-1}) of the first set of data results in a slow decomposition rate over a broad range of temperatures. In the second case (activation energy of 181 kJ mol^{-1}), the reaction activity is mainly explicated along the high-temperature (tail) region of the weight loss curves. From the quantitative point of view, the overlap between the different reaction zones is reduced passing from the first to the second kinetic evaluation, in this way resulting in significant changes in the actual chemical composition of the pseudo-components.

The applicability of more simplified kinetic models has also been evaluated in predicting the dynamics of wood weight loss at different heating rates. One-step mechanisms, using literature values for the kinetic constants, produce large errors on either the conversion time (activation energy of 103 kJ mol^{-1}) or the maximum devolatilization rate (activation energy of 149 kJ mol^{-1}). These also increase as the thermal conditions become successively more severe. Thus, a two-step mechanism, consisting of two parallel reactions, with activation energies of 147 and 149 kJ mol^{-1} , has been proposed. It has been found that, though the accuracy in predicting the details of the rate curves is worsened compared with the proposed three-step model, global devolatilization parameters are always well predicted.

This study represents one of the very few attempts to incorporate the effects of the heating rate on the global kinetics of wood devolatilization. The range of values examined ($3\text{--}108 \text{ K min}^{-1}$) is much wider than those usually employed in thermogravimetric analysis and is also of some interest in relation to practical conversion systems. Indeed, contrary to the general belief, it has been observed [24,25] that internal

heat transfer is controlling even for the small-sized particles of fast pyrolysis carried out by means of fluidized-bed reactors, so that the actual particle heating rates are always quite low. Future research, however, should be carried out to further extend the range of heating conditions and describe the behavior of biomasses other than wood by kinetic models.

References

- [1] M.G. Gronli, G. Varhegyi, C. Di Blasi, *Ind. Eng. Chem. Res.* 41 (2002) 4201–4208.
- [2] M.J. Antal, G. Varhegyi, *Ind. Eng. Chem. Res.* 34 (1995) 703–717.
- [3] G. Varhegyi, M.J. Antal, E. Jakab, P. Szabo, *J. Anal. Appl. Pyrolysis* 42 (1997) 73–87.
- [4] M.G. Gronli, A theoretical and experimental study of the thermal degradation of biomass, Ph.D. thesis, NTNU, Trondheim, Norway, 1996.
- [5] J.J.M. Orfao, F.J.A. Antunes, J.L. Figueiredo, *Fuel* 78 (1999) 349–358.
- [6] R. Bilbao, A. Millera, J. Arauzo, *Thermochim. Acta* 143 (1989) 149–159.
- [7] L. Helsen, E. Van den Bulck, *J. Anal. Appl. Pyrolysis* 53 (2000) 51–79.
- [8] J.A. Caballero, J.A. Conesa, R. Font, A. Marcilla, *J. Anal. Appl. Pyrolysis* 42 (1997) 159–175.
- [9] H. Teng, Y.C. Wei, *Ind. Eng. Chem. Res.* 37 (1998) 3806–3811.
- [10] S. Volker, T. Rieckmann, in: A.V. Bridgwater (Ed.), *Progress in Thermochemical Biomass Conversion*, Blackwell Science, 2001, pp. 1076–1090.
- [11] J.J. Manya, E. Velo, L. Puigjaner, *Ind. Eng. Chem. Res.* 42 (2003) 434–441.
- [12] J.A. Conesa, A. Marcilla, J.A. Caballero, R. Font, *J. Anal. Appl. Pyrolysis* 58–59 (2001) 617–633.
- [13] C. Di Blasi, C. Branca, *Ind. Eng. Chem. Res.* 40 (2001) 5547–5556.
- [14] C. Branca, C. Di Blasi, *J. Anal. Appl. Pyrolysis* 67 (2003) 207–219.
- [15] F. Shafizadeh, P.P.S. Chin, *Thermal deterioration of wood*, ACS Symp. Ser. 43 (1977) 57.
- [16] C.A. Koufopoulos, G. Maschio, A. Lucchesi, *Can. J. Chem. Eng.* 67 (1989) 75–84.
- [17] C. Branca, C. Di Blasi, H. Horacek, *Ind. Eng. Chem. Res.* 41 (2002) 2104–2114.
- [18] P.T. Williams, S. Besler, *Fuel* 72 (1993) 151.
- [19] M.J. Antal, G. Varhegyi, E. Jakab, *Ind. Eng. Chem. Res.* 37 (1998) 1267–1275.
- [20] F. Shafizadeh, in: R.P. Overend, T.A. Milne, L.K. Mudge (Eds.), *Fundamentals of Biomass Thermochemical Conversion*, Elsevier, London, 1985, pp. 183–217.
- [21] C. Di Blasi, *AIChE J.* 50 (2004) 2306–2319.
- [22] A. Galgano, C. Di Blasi, *Combust. Flame* 139 (2004) 16–27.
- [23] C. Di Blasi, *Polym. Int.* 49 (2000) 1133–1146.
- [24] C. Di Blasi, *AIChE J.* 48 (2002) 2386–2397.
- [25] C. Di Blasi, C. Branca, *Energy Fuel* 17 (2003) 247–254.